Journal of Cellular Biochemistry 91:880–895 (2004)

Tau Isoforms Which Contain the Domain Encoded by Exon 6 and Their Role in Neurite Elongation

Min-hua Luo,[1,2] Michael L. Leski,[3] and Athena Andreadis[1,4]*

[1]Neurobiology of Developmental Disorders, Shriver Center for Mental Retardation, Waltham, Massachusetts 02452
[2]Department of Microbiology, Xiangya Medical School, Central South University, Changsha 410078, Hunan, P.R. China
[3]Department of Psychiatry, McLean Hospital, Harvard Medical School, Worcester, Massachusetts 01655
[4]Department of Cell Biology, University of Massachusetts Medical School, Worcester, Massachusetts 01655

Abstract The regulation of tau protein expression during different stages of cellular differentiation and development as well as its functional role in morphogenesis, neurofibrillary tangle formation, and neurodegeneration have been topics of extensive study but have not been completely clarified yet. Tau undergoes complex regulated splicing in the mammalian nervous system. Our previous study with tau exon 6 demonstrated that it shows a splicing regulation profile which is distinct from that of the other tau exons as well as a unique expression pattern which is spatially and temporally regulated. In this study, we investigated the expression, localization, and effects of tau isoforms which contain exon 6 in neuroblastoma cells which stably overexpress them. We found that expression of one particular combination of tau exons (the longest adult isoform plus the domain of exon 6) significantly inhibits neurite elongation. J. Cell. Biochem. 91: 880–895, 2004.

Key words: MAP tau; alternative splicing; isoform variants; isoform localization in SH-SY5Y cells; neurite elongation

Tau is a microtubule (MT) associated protein (MAP) that promotes MT assembly and stabilizes the MT track [Hirokawa, 1994]. Tau produces multiple isoforms which are temporally and spatially regulated by utilizing two polyadenylation sites, extensive alternative splicing, and differential phosphorylation. During development, tau undergoes a transition from immature to mature forms which involves a dramatic increase in isoform number [Maccioni et al., 1995].

Tau is encoded by a single copy gene [Himmler, 1989]. It produces three transcripts of 2, 6, and 9 kb which are differentially expressed and localized in the nervous system, depending upon stage of neuronal maturation and neuron type [Goedert et al., 1989a,b; Wang et al., 1993; Nuñez and Fischer, 1997]. The 2 kb tau mRNA is localized to the nucleus [Wang et al., 1993]. The 9 kb tau transcript is restricted to the adult retina and peripheral nervous system and exclusively contains the very long exon 4A, giving rise to a tau isoform that has a size of ~110 kD [reviewed in Nuñez and Fischer, 1997]. The three tau transcripts undergo complex alternative splicing: 6 of the 16 tau exons are regulated cassettes [Goedert et al., 1989a,b; Himmler, 1989; Himmler et al., 1989; Kosik et al., 1989; Andreadis et al., 1992; Gao et al., 2000].

The N-terminus of the tau protein interacts with the plasma membrane [Brandt et al., 1995]. The middle region of the tau protein dictates MT spacing [Chen et al., 1992; Frappier et al., 1994]. The C-terminus of the tau protein contains four imperfect repeats (encoded by exons 9–12) which act as MT binding domains [Lee et al., 1989]. Exon 10 is a cassette which codes for a complete additional MT binding domain. Its inclusion increases the affinity of tau for MTs [Lee et al., 1989]. Splicing of exon 10 is under developmental and cell type-specific

Grant sponsor: NIH PO1; Grant number: HD05515.

*Correspondence to: Athena Andreadis, Shriver Center/UMMS, 200 Trapelo Rd., Waltham, MA 02452.
E-mail: Athena.Andreadis@umassmed.edu

Received 10 November 2003; Accepted 6 January 2004
DOI 10.1002/jcb.20029

regulation. Exon 10 is adult-specific in rodents and humans [Goedert et al., 1989a,b; Kosik et al., 1989] but with a crucial difference relevant to neurodegeneration: in adult rodents, exon 10 becomes constitutive [Kosik et al., 1989]. In contrast, in adult humans exon 10 remains regulated in the central nervous system [Goedert et al., 1989b; Gao et al., 2000]. The difference most likely arises from the details of the cis sequences flanking exon 10 in various organisms [Grover et al., 1999; Poorkaj et al., 2001], which in turn affect the regulation exerted by trans factors.

Tau is enriched in axons of mature and growing neurons [Kempf et al., 1996]. Tau has also been found in the cell nucleus [Wang et al., 1993], the distal ends of growing neurons [DiTella et al., 1994; Black et al., 1996] and oligodendrocytes [LoPresti et al., 1995; Gorath et al., 2001]. Tau is required for neurite outgrowth [Caceres and Kosik, 1990; Caceres et al., 1991; Liu et al., 1999], and tau dysfunction can cause neurite retraction [Nuydens et al., 1997; Sayas et al., 1999].

Hyperphosphorylated tau protein dissociated from MTs is the major component of neurofibrillary tangles, hallmark structures of dementias [Mandelkow et al., 1995; Lovestone and Reynolds, 1997]. Errors in the splicing regulation of tau exon 10, which codes for an additional MT binding domain, cause frontotemporal dementia with Parkinsonism (FTDP-17) [Clark et al., 1998; Hutton et al., 1998; Spillantini et al., 1998; D'Souza et al., 1999; Gao et al., 2000]. Also, tau null mice exhibit muscle weakness and learning defects [Ikegami et al., 2000] and their hippocampal neurons do not mature properly [Dawson et al., 2001]. Thus, tau is important to both development and maintenance of the nervous system.

Besides being misregulated in dementia, tau is also increasingly implicated in apoptosis. Very early in that process, tau is cleaved to its N-terminal fragment [Bahr and Vicente, 1998; Canu et al., 1998; Chung et al., 2001]. Experiments suggest that tau is not only a marker but also an effector for neuronal apoptosis [Fasulo et al., 2000; Zhang and Johnson, 2000]. Moreover, FTDP-17 tau mutants increase cell vulnerability to apoptosis, by disarranging the neuronal cytoskeleton [Furukawa et al., 2000; Zhao et al., 2003].

All these findings put a spotlight on the splicing of tau exon 6, which is proline-rich and, therefore, susceptible to both phosphorylation and proteolysis. A tau proline-rich domain directly downstream of exon 6 is a substrate for kinases and indispensable for MT binding [Kanai and Hirokawa, 1995; Mandelkow et al., 1995; Goode et al., 1997].

Exon 6 has been the least studied among the tau regulated exons and, until now, there has been no specific antibody targeted to its detection. By RNA methods, exon 6 has been found in both the 6 and 9 kb tau mRNAs [Himmler et al., 1989; Couchie et al., 1992]. In rodent tissues, exon 6 has been found in the mature and immature spinal cord but not in the peripheral nervous system, nor in cell lines derived from it, decoupling it from the peripheral-specific exon 4A [reviewed by Nuñez and Fischer, 1997].

Previous study by our laboratory [Wei and Andreadis, 1998; Wei et al., 2000] showed that exon 6 is not strictly a cassette, as originally believed [Himmler, 1989]. Instead, besides its canonical 3′ splice site, exon 6 utilizes two additional 3′ splice sites (Fig. 1A) [Andreadis et al., 1993; Wei and Andreadis, 1998]. The canonical exon 6 is found in low amounts in fetal human brain, and both it and its splicing variants are prominent in adult spinal cord and skeletal muscle [Wei and Andreadis, 1998]. Use of the two alternative splice sites results in frameshifts which create stop codons within or just after exon 6 [Andreadis et al., 1993]. At least one of these variant splice sites gives rise to a truncated tau isoform which is apparently expressed in normal neuronal tissue but de facto cannot bind MTs [Luo et al., submitted].

In contrast to the truncated variant, which contains only a short carboxy-terminal portion of exon 6, the tau isoforms which contain the entire exon 6 result in longer tau proteins which contain the MT binding domain. In this study, we report on the tissue expression and cellular localization of tau isoforms that contain intact exon 6 and the effect of their overexpression on neurite formation.

MATERIALS AND METHODS

Plasmid Construction

The nucleotide and amino acid sequence of tau exon 6 are shown in Figure 1A; its sequence in three mammalian species is shown in Figure 1B. The FLAG tagged and GFP tagged tau constructs are diagrammed in Figure 2A,F. The

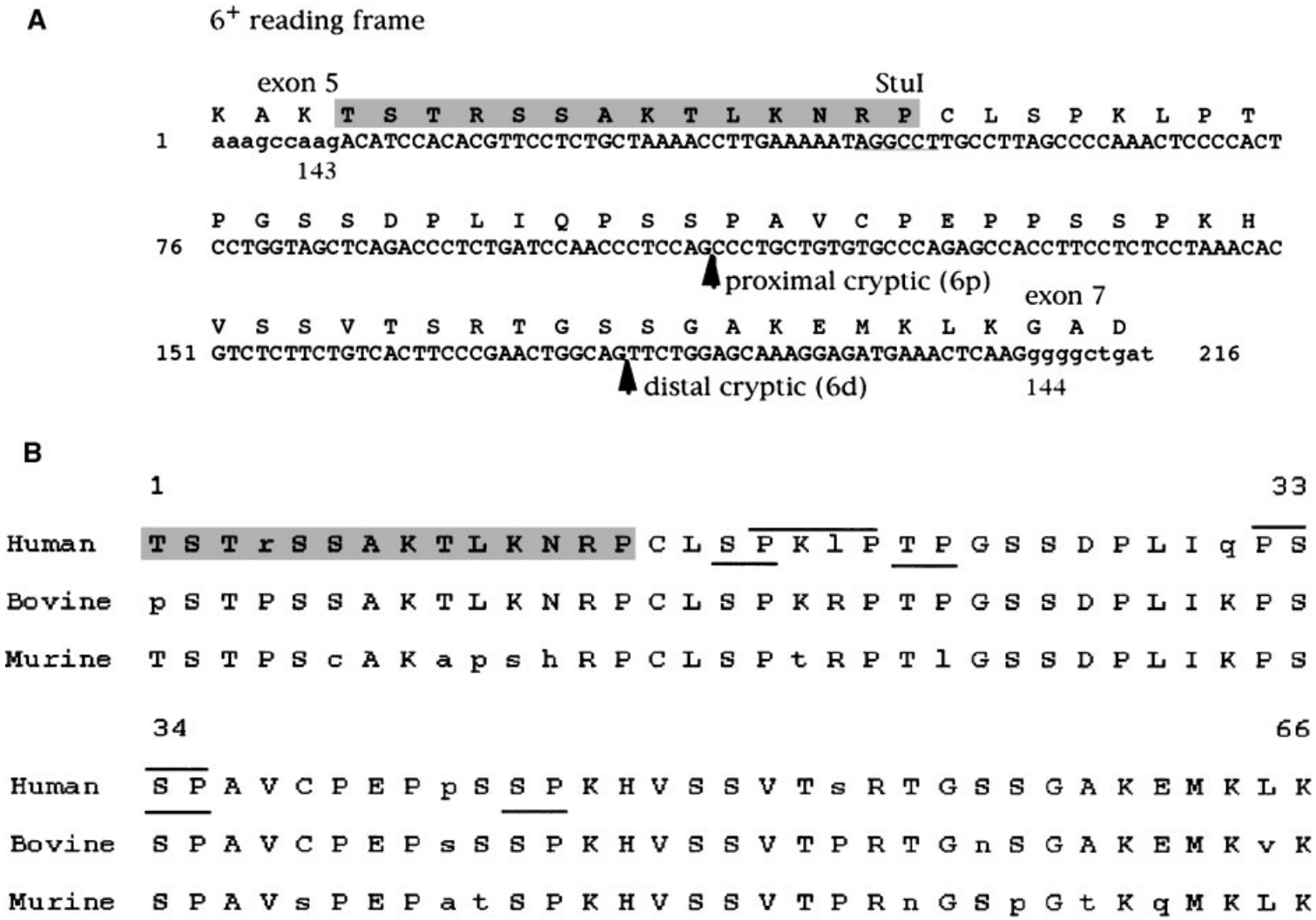

Fig. 1. Exon 6 alternative splicing variants and conservation of exon 6 in mammalian species. The shaded peptide in both panels highlights the HT6^{+} antigen. **A**: Reading frame resulting from use of the exon 6 splice site. The two arrows show the positions of the two cryptic 3′ splice sites. The StuI site is underlined. The flanking exons are indicated in lowercase. The numbers underneath exons 5 and 7 correspond to the amino acid numbers of the longest tau isoform. **B**: Amino acid sequence comparison of exon 6 between human, bovine, and murine tau. Residues conserved in all three, or in two out of the three tau species are in uppercase; residues which differ in one species or in all three are in lowercase. Phosphorylation motifs are indicated by a line above (for P-X-X-P) and below (for S/T-P) the sequence.

primers used to construct or confirm the constructs are listed in Table I.

The starting vector for the FLAG constructs was pRc/CMV/FLAG/tau, which contains the tau $2^-3^-10^+$ isoform fused at its N-terminus to the FLAG peptide. The vector also contains the *neomycin* gene under the control of the SV40 early promoter.

To generate the fetal-specific version of tau, we excised the region of pRc/CMV/FLAG/tau which contains tau exon 10 (by digestion with SacII + NheI, unique sites located in exons 7 and 13, respectively) and substituted the equivalent region from the fetal tau cDNA, thus removing exon 10 but reconstituting the rest of tau. This created FLAG-fused fetal tau (FFT/6^-), which lacks exons 2, 3, and 10.

To generate the longest adult-specific version of tau, we excised the region of pRc/CMV/FLAG/tau which borders exons 2 and 3 (by digestion with EspI + BbrPI, unique sites located in exons 1 and 4, respectively) and substituted the equivalent region from the adult 2^+3^+ tau cDNA, thus inserting exons 2 and 3 and reconstituting the rest of tau. This created FLAG-fused adult tau (FAT/6^-), which contains exons 2, 3, and 10.

To generate the 6^+ variants, we used total RNA from SKN-SH cells as a template for reverse transcription and nested PCR (the first primer pair was HT4S/HT9N3, the second HT4S3/HT7N, giving products which start in exon 4 and end in exon 7). The PCR product of the correct size was cloned into pCRII Topo-TA (Invitrogen, Carlsbad, CA), resulting in plasmid TOPO/6^+. We then excised the region of FAT/6^- and FFT/6^- which flanks exon 6 (by digestion with BbrPI and SacII, unique sites located in exons 4 and 7, respectively) and substituted the equivalent region from TOPO/6^+, thus creating FAT/6^+ and FFT/6^+.

To generate the GFP constructs, we digested expression vector EGFP-C3 (Clontech, Palo Alto, CA), with AccI (5′ end) and ApaI (3′ end); we chose C3 because it creates a continuous reading frame between GFP and tau. We obtained the entire tau inserts from the FLAG/tau constructs by digestion with ClaI and ApaI (unique sites which flank the tau cDNA at its 5′ and 3′ end, respectively; ClaI generates cohesive ends compatible with AccI). In this manner we created GFP-tagged adult tau with and without exon 6 (GAT/6^+, GAT/6^-) and GFP-tagged fetal tau with and without exon 6 (GFT/6^+, GFT/6^-).

For all constructions, the DNA fragments were run on agarose gels and extracted by the GeneClean method (kit III, Biogene, Carlsbad, CA). We confirmed the identities of the various constructs by PCR (primer pairs were HT1S/HT7N, HT4S/HT6N3, and EGFP-S/HT6N3 shown in Table I) and by sequencing in an automatic fluorescent ABI Prism sequencer.

Cell Culture, Transfections, and Lysate Preparation

COS cells (monkey kidney) and SH-SY5Y cells (human neuroblastoma, henceforth SY5Y, a generous gift from Paul Mathews, Nathan Kline Institute, NY) were maintained in Dulbecco's modified Eagle medium supplemented with 10% FCS.

Plasmid DNA was purified by cesium chloride banding. Ten μg or microgram of FLAG-tau or GFP-tau plasmids were introduced into the cells by the lipofection method (LT1, Invitrogen). The medium was changed 16 h after transfection, without glycerol shock. Cells were harvested 48 h post-transfection.

To prepare protein lysates for Western blotting, the cells were washed with phosphate-buffered saline (PBS, Invitrogen), suspended in lysis buffer (50 mM Tris pH 7.5, 1 mM EDTA, 0.5% NP40, 10% Glycerol, 150 mM NaCl, 2 mM DTT) containing 1× protease inhibitor cocktail (Boehringer Ingelheim GmbH, Germany),

Fig. 2. FLAG- and GFP-tagged tau constructs and their expression in COS and SY5Y cells, respectively. **A**: Diagram of expressed FLAG-tagged tau isoforms. The FLAG epitope and the regulated tau exons are delineated by symbols indicated on the right of the constructs. The predicted and observed sizes of the isoforms are listed below the diagrams. **B–E**: Western blots of lysates of transiently transfected COS cells transfected with constructs indicated in (A). 30 (B, C) or 50 μg (D, E) of cell lysate were run on 10% SDS–PAGE. Primary antibodies used are indicated on the left side of each panel, protein markers on the right. The proteins produced by the constructs were detected with (B) monoclonal anti-FLAG (M2), (C) monoclonal tau5, (D) monoclonal 5A6, and (E) polyclonal HT6 antibody. **F**: Diagram of expressed GFP-tagged tau isoforms. The construct conventions are identical to those in (A). The predicted and observed sizes of the isoforms are listed below the diagrams. **G** and **H**: Western blots of lysates of stably transfected SY5Y cells transfected with constructs indicated in (F). Fifty μg or micrograms of cell lysate were run on 10% SDS–PAGE. Protein markers are indicated at right. The proteins produced by the constructs were identified with (G) monoclonal anti-GFP and (H) monoclonal 5A6 antibody.

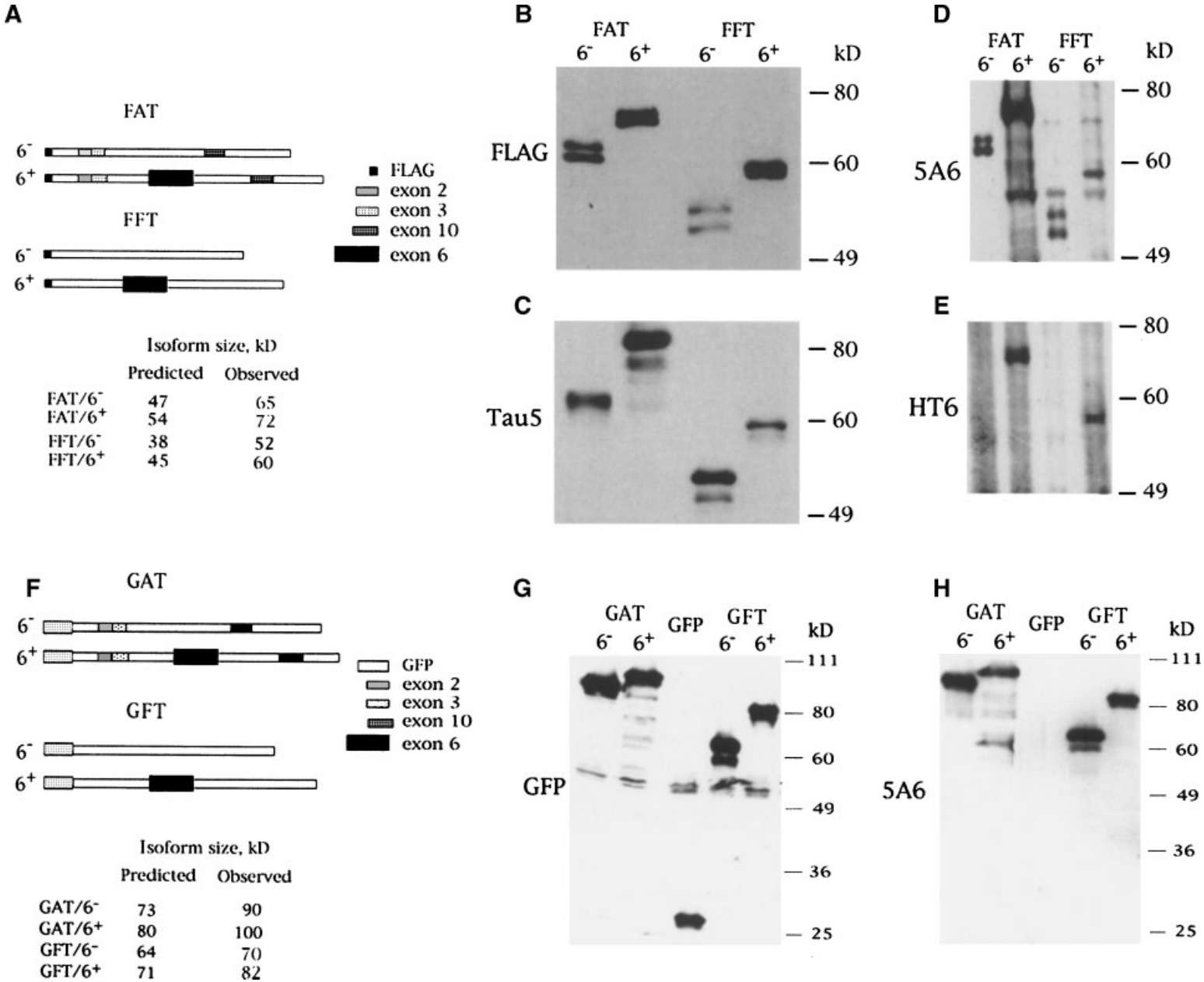
A
FAT
6-
6+
FFT
6-
6+
FLAG
exon 2
exon 3
exon 10
exon 6
Isoform size, kD
Predicted Observed
FAT/6- 47 65
FAT/6+ 54 72
FFT/6- 38 52
FFT/6+ 45 60
B
FAT FFT
6- 6+ 6- 6+
kD
FLAG
80
60
49
C
Tau5
80
60
49
D
FAT FFT
6- 6+ 6- 6+
kD
5A6
80
60
49
E
HT6
80
60
49
F
GAT
6-
6+
GFT
6-
6+
GFP
exon 2
exon 3
exon 10
exon 6
Isoform size, kD
Predicted Observed
GAT/6- 73 90
GAT/6+ 80 100
GFT/6- 64 70
GFT/6+ 71 82
G
GAT GFP GFT
6- 6+ 6- 6+
kD
GFP
111
80
60
49
36
25
H
GAT GFP GFT
6- 6+ 6- 6+
kD
5A6
111
80
60
49
36
25

Fig. 2.

TABLE I. Primers Used in Construct Generation and Identification

Names	Length	Orientation	Sequences	Location
HT1S	20	Sense	AACCAGGATGGCTGAGCCCC	Within exon 1
HT4S	20	Sense	TGAAGAAGCAGGCATTGGAG	Within exon 4
HT4S3	21	Sense	GACGAAGCTGCTGGTCACGTG	Within exon 4
HT6N3	24	Antisense	CTTAGATTTCATCTCCTTTGCTCC	Within exon 6
HT7N	20	Antisense	ATCCTGGTGGCGTTGGCCTG	Within exon 7
HT9N3	24	Antisense	CACCTTCCCGCCTCCCGGCTGGTG	Within exon 9
EGFP-S	24	Sense	GGTCCTGCTGGAGTTCGTGACCGC	In EGFP vector

sonicated and boiled for 10 min. To prepare RNA for reverse transcription and PCR, RNA was extracted by the TRIzol method (Invitrogen).

Reverse Transcription and PCR Reactions

To obtain the exon 6 cDNA, we reverse-transcribed 5 μg of total RNA from SKN cells using RNAase H^- Superscript (Invitrogen), in 20 μl for 1 h at 42°C. Three μl or microliters of this reaction mix underwent PCR after addition of two Ready-to-Go PCR beads (Amersham Biosciences, Piscataway, NJ) in a total volume of 50 μl (with primer pair HT4S/HT9N3). Five microliter of the first PCR reaction underwent a second PCR after addition of two Ready-to-Go PCR beads in a total volume of 50 μl (with nested primer pair HT4S3/HT7N). The PCR conditions were: denaturation 94°C/1 min, annealing 58°C/1 min, and extension 72°C/1 min, 30 cycles.

Western Blotting

To detect transfected tau in cells, cell protein lysates were quantified by the Bio-Rad DC protein assay. We ran 30 or 50 μg of each lysate on 10% SDS–PAGE gels, then transferred them to 0.45 μm nitrocellulose membranes (GE Osmonics, Minnetonka, MN Fig. 2).

To detect the distribution of both canonical tau and of $HT6^+$ isoforms in tissues, 100 μg of various human protein medleys (Clontech) were run on 8% SDS–PAGE (fetal brain, whole adult brain, cerebellum, cortex, hippocampus, thalamus, spinal cord, skeletal muscle, and liver as negative control; each medley represents 8–63 individuals; Fig. 3).

The membranes were blocked in TBST (20 mM Tris pH 7.5, 150 mM NaCl, and 0.05% Tween 20) containing 5% nonfat dry milk for 2 h at room temperature. The membranes were incubated with primary antibodies for 1.5 h at room temperature, washed with TBST (3×, 10 min); incubated with horseradish peroxidase conjugated secondary antibodies for 1 h, washed with TBST (5×, 10 min); and finally developed with chemiluminescence reagents (ECL, Amersham Pharmacia Biotech).

The following antibodies were used as primaries: anti-FLAG M2 monoclonal (Sigma-Aldrich, St. Louis, MO) at 1:5,000 dilution, anti-GFP monoclonal (Zymed Laboratories, SanFrancisco, CA) at 1:5,000, anti-tau monoclonal Tau5 (a generous gift of Skip Binder) at 1:10,000, anti-tau monoclonal 5A6 (which recognizes residues 20–46; a generous gift of Gloria Lee) at 1:5,000, and anti-HT6 polyclonal at 1:500; as secondaries, goat anti-mouse and anti-rabbit (Zymed) at 1:50,000. Anti-HT6 is an affinity-purified polyclonal antibody raised in rabbit against the human tau exon 6 peptide TSTRSSAKTLKNRP (generated and affinity-purified by Zymed; the epitope peptide is shown shaded in Fig. 1). This antibody can only recognize the intact exon 6 domain; exon 6 splicing variants do not contain this region (Fig. 1A).

Establishment of Stably Transfected cell Lines

To create stable cell lines, the medium of SY5Y cells was changed 16 h after transfection. Cells were passed and selected with 500 μg/ml G418 (Invitrogen) until colonies were visible after 15 days; the medium was changed every 3 days. Colonies which showed green fluorescent signal were picked out by trypsinization within cloning cylinders (Bel-Art Products, Pequannock, NJ), transferred to 12-well plates and maintained in medium containing 500 μg/ml G418. Each of these colonies was tested for expression of the FLAG/tau and GFP/tau constructs by Western blotting. Those colonies which showed strong signals both in Western blots and (for GFP) green fluorescence were subsequently differentiated with all-trans retinoic acid (RA, Sigma).

Differentiation of the Stably Transfected SY5Y Cells by Retinoic Acid

SY5Y cells stably transfected with tau constructs were transferred to poly-D-lysine coated

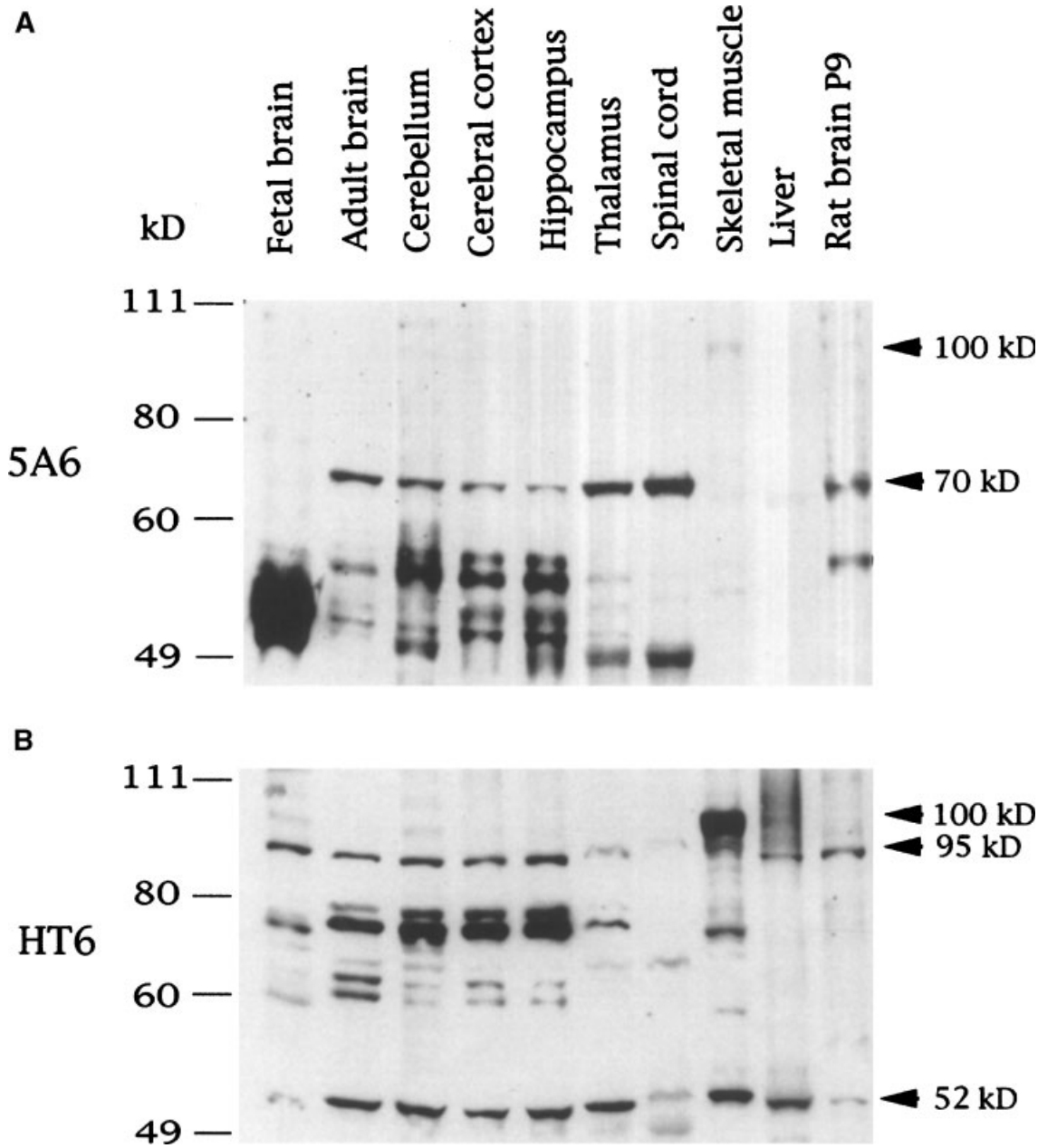

Fig. 3. Endogenous expression of tau canonical and 6^+ variants in human tissues. 100 μg of human protein medleys were applied to a 8% SDS–PAGE gel. Primary antibodies used are indicated on the left side of each panel, protein markers on the right. Western blots of endogenous **(A)** canonical tau detected by monoclonal 5A6 antibody and **(B)** 6^+ tau detected by polyclonal HT6 antibody.

slide chambers (Nalge Nunc Intl., Rochester, NY) at an initial density of 1×10^4 cells/cm^2. RA was added the day after plating at a final concentration of 10 μM in DMEM with 10% FCS and 500 μg/ml G418. RA and medium were changed every 2 days. After 14 days of RA treatment, cytosine β-D arabinoside (AraC, Sigma) was added at a final concentration of 40 μM, and cells were treated with both RA and AraC for at least 7 additional days.

Immunocytochemistry

For images of living cells, the cells were plated in poly-D-lysine coated slide chambers

(Lab-Tek, Nalge Nunc) and differentiated with RA for 2 weeks as described above. Cells were rinsed 3× with NL buffer (154 mM NaCl, 5.6 mM KCl, 1 mM $MgCl_2$, 2.3 mM $CaCl_2$, 3.6 mM $NaHCO_3$, 5 mM HEPES, 5.6 mM D-glucose). Then 1 ml of NL was added to the wells and the cells were observed under a confocal microscope.

For images of fixed cells, the slides carrying differentiated stable expressing SY5Y cells were rinsed twice with PBS, then fixed for 1 h at room temperature in PBS containing 2% (v/v) paraformaldehyde and 0.1% glutaraldehyde, washed with PBS, permeabilized with 0.1% Triton X-100 in PBS for 30 min, and incubated with 0.1 M glycine in PBS for 20 min. After fixation and permeabilization, slides were blocked in PBS containing 1% bovine serum albumin (BSA) at room temperature for 1 h.

For extraction of non-cytoskeletal associated tau, the cells were first rinsed with PBS and then with extraction buffer (80 mM PIPES/KOH pH 6.8, 1 mM $MgCl_2$, 1 mM EGTA, 30% glycerol, 1 mM GTP). The cells were subsequently extracted with 0.02% saponin in extraction buffer for 30 s, then washed with extraction buffer at 37°C. The cells were then fixed for 1 h at room temperature with 2% paraformaldehyde, 0.1% glutaraldehyde in extraction buffer, washed with PBS, permeabilized with 0.1% Triton X-100 in PBS for 30 min, washed with PBS, and incubated with 0.1 M glycine in PBS for 20 min. Following fixation, cells were blocked with 1% BSA in PBS for 1 h.

The antibodies were diluted in PBS containing 1% BSA and were: as primaries, monoclonal anti-FLAG (M2) IgG (Sigma) at 1:500 dilution and anti-α-tubulin IgG (Zymed) at 1:100 dilution. As secondaries, respectively, Cy3-labeled anti-mouse IgG (Accurate Chemical & Scientific Corporation, Westburg, NY) at 1:200 dilution and Cy5-labeled anti-mouse IgG (Zymed) at 1:500 dilution. Staining with primary antibody was done for 1 h at RT, with secondary antibody for 30 min. Slides were mounted with mounting solution (Biomeda, Foster City, CA) and observed under a confocal fluorescent microscope. Confocal image analysis used a Leica TCS 4D true confocal scanner, with layers comprising a thickness of 1 μm.

The length of the neurites was measured from the confocal immunofluorescence micrographs of the differentiated cells which stably expressed GFP constructs and showed the GFP fluorescence signal. The length was measured by following the signal of the anti-α tubulin antibody, using software IPLab 3.5.

RESULTS

Expression of the FLAG and GFP Tagged Tau Variants in COS and SY5Y Cells

To determine if the constructs (Fig. 2A,F) express correctly, we introduced them into COS cells. The Western blotting results show that both the FLAG and GFP tagged tau variants constructs express the full-length tau isoforms in equivalent amounts.

Figure 2B–D show the expression of the FLAG tagged human tau isoforms in COS cells as visualized by FLAG, tau5, 5A6, and HT6 antibodies. Tau5 recognizes an epitope in exon 9 and 5A6 an epitope in exon 1 of tau (amino acid residues 211–230 and 20–46, respectively of the 441 residue longest tau isoform) [Johnson et al., 1997]. Figure 2E shows that the anti-HT6 antibody is specific, as it recognizes only the 6^+ isoforms (second and fourth lane) but not the 6^- isoforms (first and third lane).

Subsequently, all eight constructs were introduced into SY5Y human neuroblastoma cells to establish stable cell lines. We were able to establish stable cell lines for all the constructs except FAT/6^+. The sizes of the stably expressed proteins in SY5Y cells are identical to those of the transiently expressed proteins in COS cells (COS data not shown). Figure 2G,H show the expression of the GFP tagged human tau isoforms in stably expressing SY5Y cells as visualized by GFP and 5A6 antibodies.

The predicted and observed sizes of the construct proteins are listed in Figure 2A,F. The 6^+ variants are larger than their 6^- counterparts by approximately 10 kD, consistent with the size of the exon 6 peptide (which consists of 66 amino acids). The difference between predicted and observed sizes and the doublet seen by most of the antibodies are due to phosphorylation. The bands from each construct collapse to a singlet of the correct size when dephosphorylated (data not shown).

Presence and Distribution of the 6^+ Isoform in Tissue Lysates

To determine the gamut of endogenous tau isoforms in different tissues, 100 μg of human protein medleys (each representing 8–63 indi-

viduals; Clontech) were subjected to Western analysis with an antibody to total tau (monoclonal 5A6, Fig. 3A) and with the antibody we raised against the start of human tau exon 6 (polyclonal anti-HT6, Fig. 3B).

In adult human brain tissues (whole brain, cerebellum, cortex, hippocampus), the 5A6 antibody picked up the expected and characteristic tau sextet ladder of 50–60 kD (Fig. 3A). Cerebellum, cortex, and hippocampus show equivalent amounts of signal, whereas the signal is weaker in whole brain. The relative ratios of each member of the ladder differ among the four tissues. Cerebellum is the only tissue in which the largest band of the sextet is easily visible (at 60 kD). In fetal brain the strength of the signal has shifted toward the shorter members of the sextet and is centered at 55 kD (Fig. 3A, leftmost lane). In thalamus and spinal cord the predominant signal is a weak band at 52 kD which corresponds to the smallest member of the sextet, whereas skeletal muscle and liver show only very faint bands—although, as we discuss in the next paragraph, we have reason to believe that the muscle band at ~100 kD is specific (Fig. 3A, upper arrow).

Intriguingly, in all adult CNS tissues (whole brain, cerebellum, cortex, hippocampus, spinal cord, and thalamus) 5A6 also picks up a band of 70 kD (Fig. 3A, lower arrow). We have seen this band consistently with 5A6 [Luo et al., submitted]; it may correspond to the elusive "medium-sized" tau described by several researchers in the field. The likelihood that the 70 kD band is specific is increased by the fact that it is also seen in rat brain, in which 5A6 recognizes band of that size as well as a 60 kD band that corresponds in size to the largest member of the human sextet seen in cerebellum (Fig. 3A, third lane from the left and rightmost lane).

Just as the anti-HT6 antibody does not recognize the 6^- isoforms of the transfected tau fusion constructs (Fig. 2E), it also does not recognize the 6^- isoforms in tissues (Fig. 3B), which is further proof of its specificity. Anti-HT6 picks no species in the region between 50 and 60 kD (the interval in which cluster the 6^- isoforms recognized by 5A6; Fig. 3A), except for a ubiquitous non-specific band at about 52 kD (Fig. 3B, lower arrow). Instead, once again a sextet appears between 60 and 80 kD. In fetal brain, the entire ladder is displaced downward relatively to its position in adult brain tissues (Fig. 3B, leftmost lane), consistent with the absence of regulated exons 2, 3, and 10 in fetal tau.

Thalamus and spinal cord show weak bands (3 and 1, respectively) corresponding in size to one or more members of the sextet. As with the species recognized by 5A6 (Fig. 3A), the relative ratios of each species differ among the brain tissues. Skeletal muscle shows the ubiquitous band at 52 kD as well as a band around 75 kD. Most interestingly, it also shows a strong band at 100 kD, which almost certainly is the peripheral-specific tau isoform that contains the domains of exons 6 and 4A (Fig. 3B, upper arrow).

With anti-HT6, neither liver nor rat brain show any bands beyond the two ubiquitous, non-specific species of 52 and 95 kD (Fig. 3B, two rightmost lanes). It is not surprising that anti-HT6 does not recognize rat exon 6, because the region which served as the epitope for anti-HT6 is not well conserved between murine and human tau (Fig. 1B; 6 out of 14 residues differ between the two species). Interestingly, antibody 5A6 does not recognize the endogenous tau species between 60 and 80 kD delineated by the anti-HT6 antibody (Fig. 3), whereas it recognizes the proteins expressed from the constructs (Fig. 2).

Localization and Effect of Exon 6 Isoforms in Stably Transfected SY5Y Cells After RA Differentiation

The SY5Y human neuroblastoma line can be differentiated to neuron-like cells [Encinas et al., 2000]. The endogenous tau in undifferentiated SY5Y cells resides predominantly in the nucleus, whereas in SY5Y cells differentiated with RA tau is found in the cell body, along the processes and at the tip of the processes [Uberti et al., 1997]. Using immunofluorescence, we examined the location of the FLAG- and GFP-tagged tau isoforms in SY5Y cells which stably express them after treatment with RA for 14 days. As mentioned previously, we were able to establish stable cell lines for all the FLAG and GFP constructs except FAT/6^+.

Figure 4 shows the localization of the stably expressed FLAG-tagged tau constructs after RA differentiation and the morphology of the SY5Y cells which express them. The FLAG signal is excluded from the nucleus and most of the cell body. All the stable lines extend long neurites, though the processes are overall shorter in the

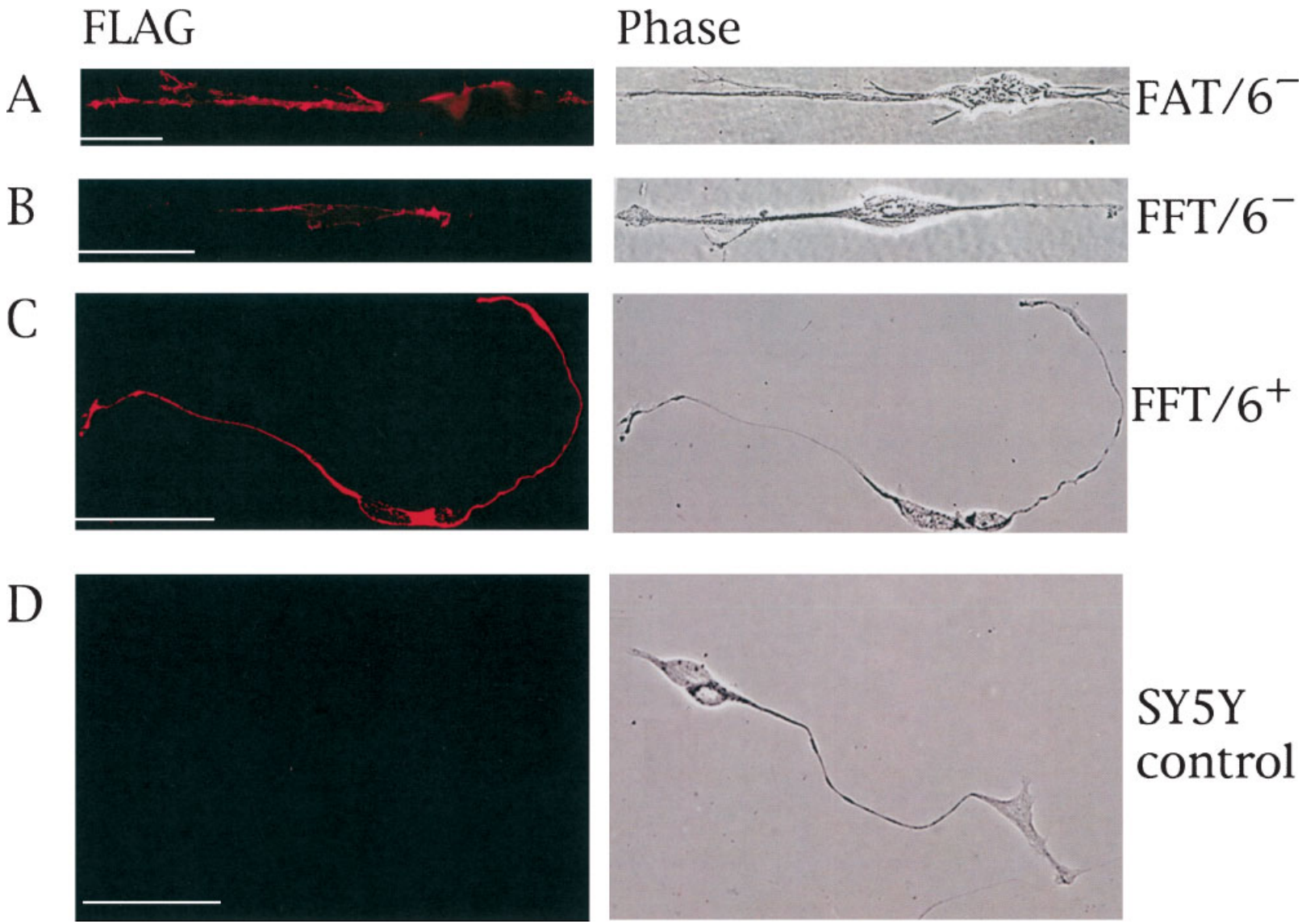

Fig. 4. Localization of FLAG-tagged tau exon 6 variants in stably transfected SY5Y cells differentiated with RA for 3 weeks. The left column shows immunofluorescence and the right column shows phase views. The expressed constructs are indicated at the right of each panel pair. Antibodies used: Primary, anti-FLAG M2 IgG; secondary, cy3-labeled anti-mouse IgG. Scale bar = 100 μm.

FFT/6^+ line. The neurites of the FFT/6^+ isoform are sometimes curved and also appear slightly dystrophic (Fig. 4C). The FFT/6^- isoform remains close to the cell body and goes only part way down the process (Fig. 4B) whereas the other two isoforms extend to the end of the processes.

Figure 5 shows the location of stably expressed GFP-tagged tau 6^- and 6^+ isoforms in the living differentiated SY5Y cells. The localization of the overexpressed GFP-tagged tau isoforms is similar whether we observe living cells (Fig. 5A–D) or after extraction (Fig. 5E). The fluorescent signal is excluded from the nucleus and is visible in the cell bodies and processes in the characteristic "network" configuration.

After RA differentiation, all the stable lines develop long processes, with one exception: the neurites of the GAT/6^+ cells are significantly shorter (Fig. 5B). Table II shows the quantitation of the neurite lengths for the differentiated SY5Y lines stably expressing GAT/6^+, GAT/6^-, and the GFP-vector. The average length of the GAT/6^+ neurites is 25% of the controls and of its 6^- counterpart. The inescapable conclusion is that overexpression of this particular isoform inhibits neurite elongation.

During cell passage and RA differentiation, the GFP-positive cell number in GAT/6^+ declined much faster than in all the other cell lines (GFP, GAT/6^-, GFT/6^-, and GFT/6^+). After 50 passages, even with continuous maintenance at 500 μg/ml G418, the green fluorescent signal of GAT/6^+ disappeared. The GAT/6^+ isoform may be toxic to the cells in large amounts (this possibility is made likelier by the fact that we were unable to establish a stable line for its FLAG counterpart, FAT/6^+); alternatively, this particular isoform may be especially subject to downregulation or proteolysis.

To ascertain whether the overexpressed GFP-tagged tau isoforms distribute themselves similarly to canonical tau, we investigated how they localize with respect to tubulin. Overlays of the GFP signal and tubulin immunofluorescence (Fig. 6) show that all the GFP-tagged isoforms co-localize with tubulin. Yet again, GAT/6^+ differs somewhat from the rest: whereas the GFP fluorescence of the other three constructs extends all the way to the end of the processes, GAT/6^+ stops short from the end (Fig. 6B).

DISCUSSION

Exon 6 Increases the Complexity of the Tau Molecule

Tissue-specific alternative splicing profoundly affects physiology, development, and disease, and this is nowhere more evident than in the nervous system [Grabowski and Black, 2001]. The *tau* gene illustrates the versatility of this mechanism: taking exon 6 splicing decisions into account, tau can theoretically produce at least 30 variants by splicing alone, not counting variations introduced by post-translational modifications.

Our previous study showed that tau exon 6 has a unique expression pattern which differs from that of all other tau regulated exons [Wei and Andreadis, 1998]. Unlike exons 2, 3, and 10, it appears in fetal brain and unlike exon 4A, it is present in the central nervous system. mRNAs containing exon 6 have been found in adult forebrain and cerebellum, juvenile and adult spinal cord and skeletal muscle [Wei and Andreadis, 1998].

The most curious aspect of exon 6 expression is the existence and utilization of the cryptic sites which give rise to frameshifts and hence to truncated tau molecules lacking the MT binding domains [Andreadis et al., 1993; Wei and Andreadis, 1998; Luo et al., submitted]. On the other hand, inclusion of exon 6 in its entirety preserves the reading frame and results in a longer tau isoform which includes the proline-rich domain encoded by this exon (Fig. 1). The 6^+ isoforms have been investigated primarily at the RNA level [Himmler, 1989; Andreadis et al., 1993; Nuñez and Fischer, 1997; Wei and Andreadis, 1998]. In this study, we examined the spatial and temporal distribution of the 6^+ protein isoforms, as well as their localization and possible function.

To aid us in our investigation, we generated an affinity-purified polyclonal antibody (anti-HT6) which recognizes the 14 amino acids at the beginning of exon 6 (shown shaded in Fig. 1). Our Westerns with 6^- and 6^+ tau constructs show convincingly that the anti-HT6 antibody does not recognize the 6^- tau species (Fig. 2). Using this specific antibody, we discovered that the tau variant which incorporates the exon 6 peptide is indeed expressed in the human central nervous system and, moreover, it is spatially and temporally regulated (Fig. 3). In particular, the exon 6 domain is present in fetal

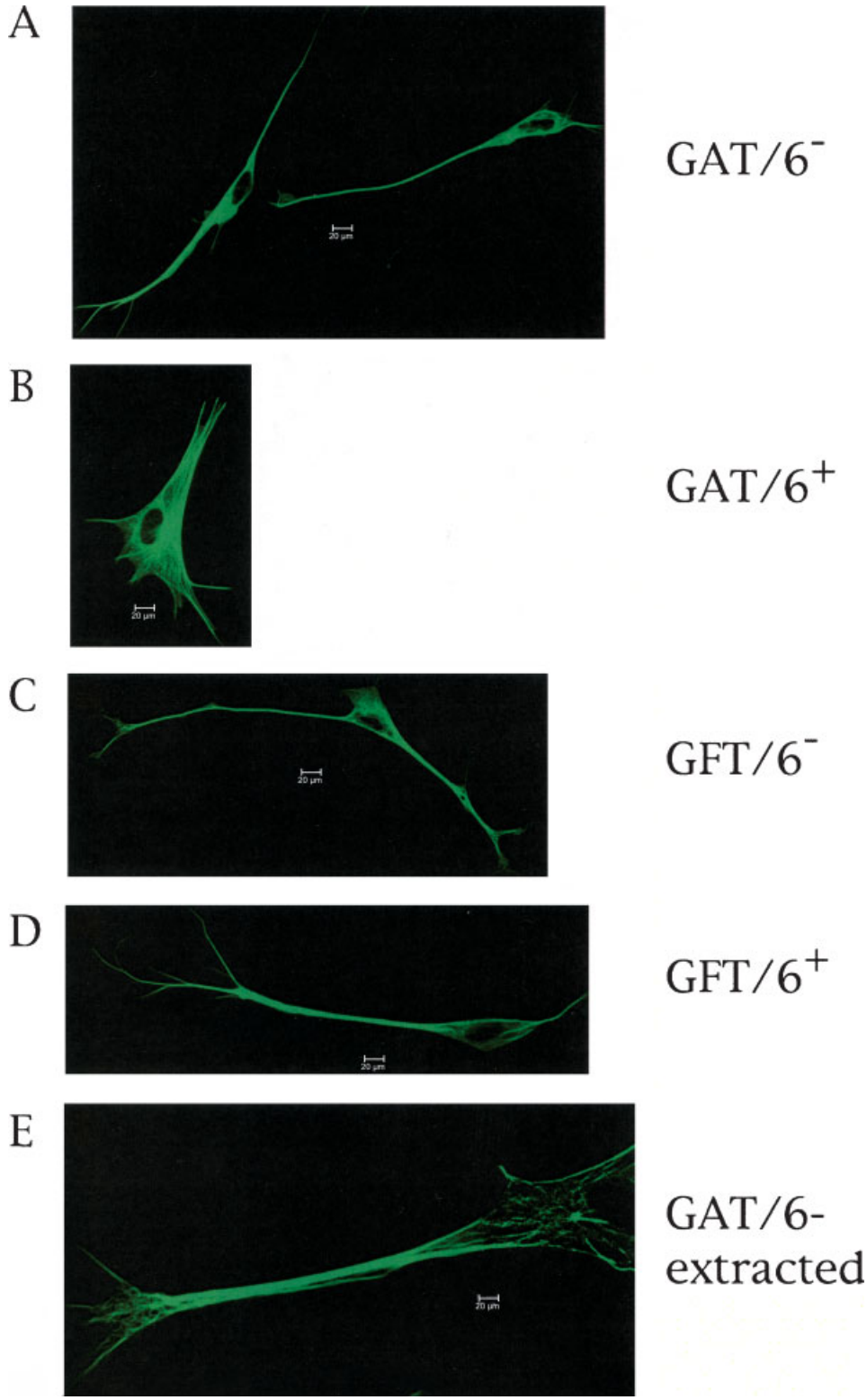

Fig. 5. Confocal fluorescence images of living and extracted SY5Y cells stably transfected with GFP-tagged tau exon 6 variants. Images were captured after 2 weeks of treatment with RA. The expressed constructs are indicated at the right of each panel. The GAT/6$^+$ line (**B**) consistently shows shorter neurites, quantitated in Table II. After extraction of the non-cytoskeletal tau, the images of all the stable cell lines are similar and the fluorescence signal is mostly located in the neurites. **Panel E**: Image of the extracted GAT/6$^-$ cell line. Scale bar = 20 μm.

TABLE II. Neurite Length of the Stably Transfected SY5Y Cell Lines Treated for 2 Weeks With RA

Construct	Total neurite length (μm)	No. of neurites analyzed	Average length of neurite (μm)
GAT/6$^-$	16,732	190	88.1 ± 13.2
GAT/6$^+$	4,711	170	27.7 ± 4.5*
GFP	19,235	230	83.6 ± 12.0
None	19,826	230	86.2 ± 14.5

The length of the neurites was measured from the confocal immunofluorescence micrographs of the differentiated cells which stably expressed GFP constructs and showed the GFP fluorescence signal. The length was measured by following the signal of the anti-α tubulin antibody, using software IPLab 3.5.
*$P < 0.01$.

tau, confirming the results from RNA work [Wei and Andreadis, 1998]. These results indicate that the tau isoform profile is even more complex than originally thought, and that fetal tau consists of more species than the single $2^-3^-10^-$ one of tradition.

The Tau 6$^+$ Isoform Inhibits Neurite Extension in SY-5Y Cells

The effects of the various exon 6 isoforms in the stable SY5Y lines that we generated show an important distinction. Interestingly, we could not establish stable lines for FAT/6$^+$. The FFT/6$^+$ isoform consistently shows neurites that appear slightly dystrophic (Fig. 4C). Finally, the processes resulting from the line expressing the GAT/6$^+$ isoform are significantly shorter than all the others (Fig. 5B and Table II) and this cell line progressively loses GFP fluorescence over time.

There are several possible explanations for this behavior: the 6$^+$ isoforms may be (1) toxic if overexpressed, or (2) not toxic in themselves; but their overexpression may perturb the ratio of tau isoforms and trigger cell death. Disturbance of the tau isoform ratio is known to cause frontotemporal dementia [Clark et al., 1998; Hutton et al., 1998; Spillantini et al., 1998; D'Souza et al., 1999], and tau seems to be part of both the cause and effect of neuronal apoptosis [Bahr and Vicente, 1998; Canu et al., 1998; Fasulo et al., 2000; Zhang and Johnson, 2000]. The presence of the exon 6 domain appears to act as an inhibitor to neurite extension (Figs. 4 and 5). The 6$^+$ isoform may act as a "graphite rod" (that is, as a moderator or retardant) in the nucleation reaction of the microtubular cytoskeleton during process formation; this is consistent with its relative high level of expression in fetal brain (Fig. 3). Alternatively, incorporation of excessive amounts of the 6$^+$ isoform in the axonal cytoskeleton may result in rigid processes which cannot respond efficiently to environmental cues.

Possible Roles of the Exon 6 Domain

The tau regulated exons have different functions, some of which are known: exon 10 increases affinity to MTs [Mandelkow et al., 1995], exon 4A alters MT spacing [Chen et al., 1992; Frappier et al., 1994], and exons 2 and 3 modulate interactions with the axonal membrane [Brandt et al., 1995]. In contrast, the functions and ligands of all the variants of exon 6 are unknown. However, its high amino acid conservation in mammals (Fig. 1B) suggests that it may interact with a specific ligand. The longer, more rigid hinge region that would result from the presence of the proline-rich exon 6 domain might alter MT spacing. In this regard, it may be significant that exon 6 is particularly prominent in spinal cord and the peripheral nervous system [Nuñez and Fischer, 1997; Wei and Andreadis, 1998], which have neurons with increased MT spacing [Frappier et al., 1994].

No experiments have yet addressed the phosphorylation status of exon 6. By visual inspection, exon 6 contains four S/T-P and two P-X-X-P motifs (Fig. 1B, under- and over-lined, respectively). The former can be phosphorylated by prolyl kinases and is recognized by isomerases such as Pin1 [Mandelkow et al., 1995; Lu et al., 1999]; the latter can be phosphorylated by src-family tyrosine kinases [Lee et al., 1998]. These modifications occur at other tau sites, leading to conformational and functional changes, particularly during neurodegeneration [Billingsley and Kincaid, 1997; Lu et al., 1999]. In terms of the effect that exon 6 has on neurite extension, it is known that tau, and its hinge region in particular, influences that parameter [Teng et al., 1993; Liu et al., 1999].

By RNA and protein analysis, the exon 6$^+$ isoforms are present in tissues, developmental stages and subcellular locations which require a dynamic neuronal cytoskeleton (fetal brain, peripheral nervous system; the neurite distal tip). Therefore, the tau isoforms which include them may be involved in neuronal plasticity and/or axonal guidance. The strong effect of

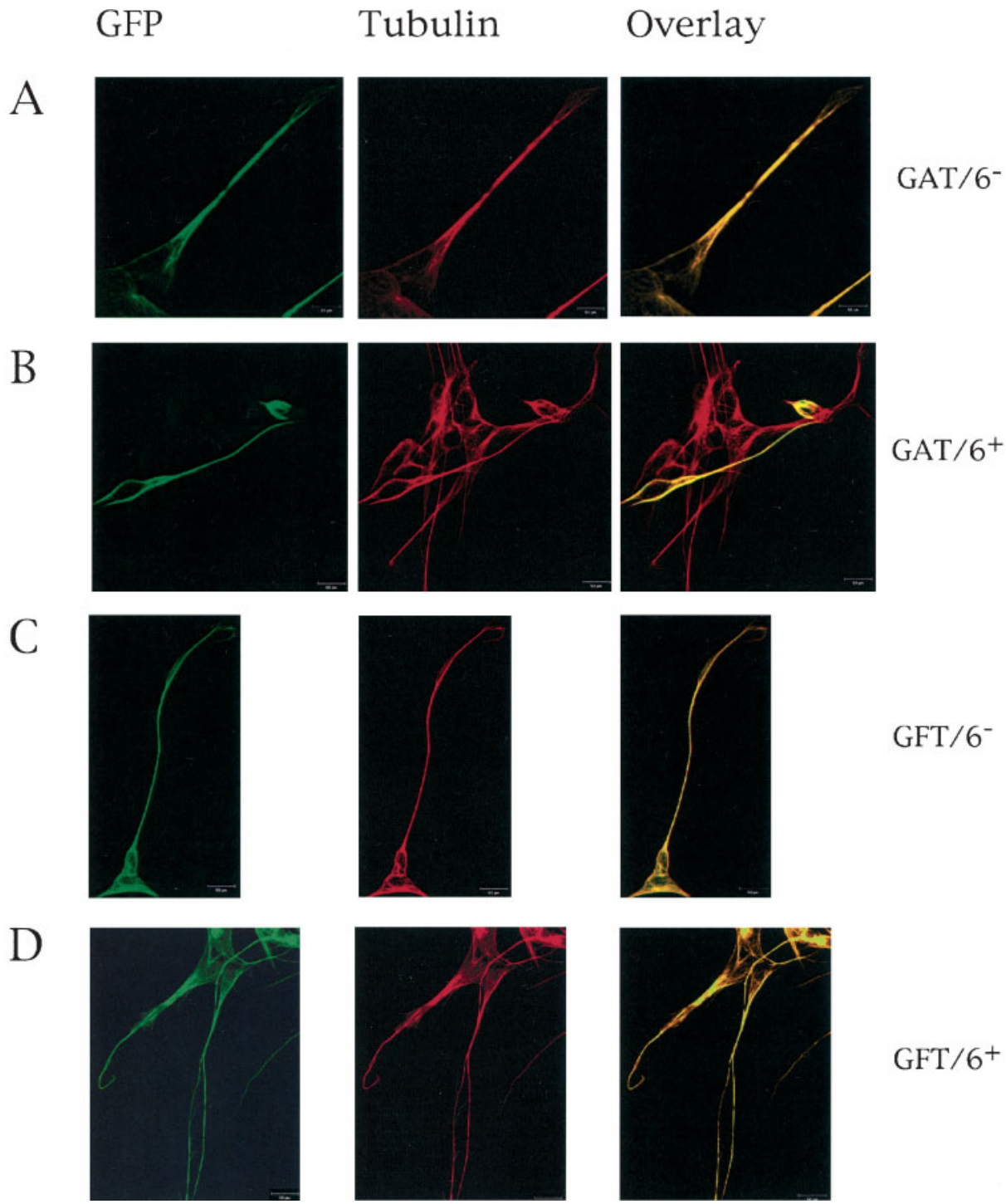

Fig. 6. Co-localization of GFP-tagged tau exon 6 variants with tubulin in stably transfected SY5Y cells differentiated with RA for 2 weeks. In each set, the **left panel** shows GFP fluorescence (green), the **middle panel** shows tubulin immunofluorescence (red), and the **right panel** shows merged images which show the co-localization of the GFP-tagged tau variants and the tubulin. The expressed constructs are indicated at the right of each panel triptych. Antibodies used: Primary, anti-α tubulin IgG; secondary, cy5-labeled anti-mouse IgG. Scale bar = 50 μm.

exon 6 overexpression on neurite morphology is compatible with a possible regulatory role. In future studies, we hope to elucidate the function and ligands of this interesting region.

ACKNOWLEDGMENTS

We thank Dr. Gloria Lee and Dr. Skip Binder for their generous gift of tau antibodies;

Dr. Denise Chou, Dr. Linda Hassinger, Dr. Jim Crandall, Dr. Fran Smith, and Dr. Stu Tobet for their precious help with microscope training; and Dr. Gloria Lee for her very helpful discussion of the article.

REFERENCES

Andreadis A, Brown WM, Kosik K. 1992. Structure and novel exons of the human *tau* gene. Biochemistry 31: 10626–10633.

Andreadis A, Nisson P, Kosik KS, Watkins P. 1993. The exon trapping assay partly discriminates against alternatively spliced exons. Nucl Acids Res 21:2217–2221.

Bahr BA, Vicente JS. 1998. Age-related phosphorylation and fragmentation events influence the distribution profiles of distinct tau isoforms in mouse brain. J Neuropathol Exp Neurol 57:111–121.

Billingsley ML, Kincaid RL. 1997. Regulated phosphorylation and dephosphorylation of tau protein: Effects on microtubule interaction, intracellular trafficking and neurodegeneration. Biochem J 323:577–591.

Black MM, Slaughter T, Moshiah S, Obrocka M, Fischer I. 1996. Tau is enriched on dynamic microtubules in the distal region of growing axons. J Neurosci 16:3601–3619.

Brandt R, Léger J, Lee G. 1995. Interaction of tau with the neural plasma membrane mediated by tau's amino-terminal projection domain. J Cell Biol 131:1327–1340.

Caceres A, Kosik KS. 1990. Inhibition of neurite polarity by tau antisense oligonucleotides in primary cerebellar neurons. Nature 343:461–463.

Caceres A, Potrebic S, Kosik KS. 1991. The effect of tau antisense oligonucleotides on neurite formation of cultured cerebellar macroneurons. J Neurosci 11:1515–1523.

Canu N, Dus L, Barbato C, Ciotti MT, Brancolini C, Rinaldi AM, Novak M, Cattaneo A, Bradbury A, Calissano P. 1998. Tau cleavage and dephosphorylation in cerebellar granule neurons undergoing apoptosis. J Neurosci 18: 7061–7074.

Chen J, Kanai Y, Cowan NJ, Hirokawa N. 1992. Projection domains of MAP2 and tau determine spacings between microtubules in dendrites and axons. Nature 360:674–677.

Chung CW, Song YH, Kim IK, Yoon WJ, Ryu BR, Jo DG, Woo HN, Kwon YK, Kim HH, Gwag BJ, Mook-Jung IH, Jung YK. 2001. Proapoptotic effects of tau cleavage product generated by caspase-3. Neurobiol Dis 8:162–172.

Clark LN, Poorkaj P, Wszolek Z, Geschwind DH, Nasreddine ZS, Miller B, Li D, Payami H, Awert F, Markopoulou K, Andreadis A, D'Souza I, Lee VM, Reed L, Trojanowski JQ, Zhukareva V, Bird T, Schellenberg G, Wilhelmsen KC. 1998. Pathogenic implications of mutations in the *tau* gene in pallido-ponto-nigral degeneration and related neurodegenerative disorders linked to chromosome 17. Proc Natl Acad Sci USA 95:13103–13107.

Couchie D, Mavilia C, Georgieff IS, Liem RKH, Shelanski ML, Nuñez J. 1992. Primary structure of high molecular weight tau present in the peripheral nervous system. Proc Natl Acad Sci USA 89:4378–4381.

D'Souza I, Poorkaj P, Hong M, Nochlin D, Lee VM, Bird TD, Schellenberg GD. 1999. Missense and silent *tau* gene mutations cause frontotemporal dementia with parkinsonism-chromosome 17 type, by affecting multiple alternative RNA splicing regulatory elements. Proc Natl Acad Sci USA 96:5598–5603.

Dawson HN, Ferreira A, Eyster MV, Ghoshal N, Binder LI, Vitek MP. 2001. Inhibition of neuronal maturation in primary hippocampal neurons from tau deficient mice. J Cell Sci 114:1179–1187.

DiTella M, Feiguin F, Morfini G, Cáceres A. 1994. Microfilament-associated growth cone component depends upon tau for its intracellular localization. Cell Motil Cytoskel 29:117–130.

Encinas M, Iglesias M, Liu Y, Wang H, Muhaisen A, Cena V, Gallego C, Comella JX. 2000. Sequential treatment of SH-SY5Y cells with retinoic acid and brain-derived neurotrophic factor gives rise to fully differentiated, neurotrophic factor-dependent, human neuron-like cells. J Neurochem 75:991–1003.

Fasulo L, Ugolini G, Visintin M, Bradbury A, Brancolini C, Verzillo V, Novak M, Cattaneo A. 2000. The neuronal microtubule-associated protein tau is a substrate for caspase-3 and an effector of apoptosis. J Neurochem 75: 624–633.

Frappier TF, Georgieff IS, Brown K, Shelanski ML. 1994. Tau regulation of microtubule-microtubule spacing and bundling. J Neurochem 63:2288–2294.

Furukawa K, D'Souza I, Crudder CH, Onodera H, Itoyama Y, Poorkaj P, Bird TD, Schellenberg GD. 2000. Proapoptotic effects of tau mutations in chromosome 17 frontotemporal dementia and parkinsonism. Neuroreport 11:57–60.

Gao QS, Memmott J, Lafyatis R, Stamm S, Screaton G, Andreadis A. 2000. Complex regulation of tau exon 10, whose missplicing causes frontotemporal dementia. J Neurochem 74:490–500.

Goedert M, Spillantini MG, Jakes R, Rutherford D, Crowther RA. 1989a. Multiple isoforms of human microtubule-associated protein tau: Sequences and localization in neurofibrillary tangles of Alzheimer's disease. Neuron 3:519–526.

Goedert M, Spillantini MG, Potier MC, Ulrich J, Crowther RA. 1989b. Cloning and sequencing of the cDNA encoding an isoform of microtubule-associated protein tau containing four tandem repeats: Differential expression of tau protein isoforms in human brain. EMBO J 8:393–399.

Goode BL, Denis PE, Panda D, Radeke MJ, Miller HP, Wilson L, Feinstein SC. 1997. Functional interactions between the proline-rich and repeat regions of tau enhance microtubule binding and assembly. Mol Biol Cell 8:353–365.

Gorath M, Stahnke T, Mronga T, Goldbaum O, Richter-Landsberg C. 2001. Developmental changes of tau protein and mRNA in cultured rat brain oligodendrocytes. Glia 36:89–101.

Grabowski PJ, Black DL. 2001. Alternative RNA splicing in the nervous system. Prog Neurobiol 65:289–308.

Grover A, Houlden H, Baker M, Adamson J, Lewis J, Prihar G, Pickering-Brown S, Duff K, Hutton M. 1999. 5′ splice site mutations in tau associated with the inherited dementia FTDP-17 affect a stem-loop structure that regulatesalternative splicing of exon 10. J Biol Chem 274:15134–15143.

Himmler A. 1989. Structure of the bovine *tau* gene: Alternatively spliced transcripts generate a gene family. Mol Cell Biol 9:1389–1396.

Himmler A, Drechsel D, Kirschner MW, Martin DW. 1989. Tau consists of a set of proteins with repreated C-terminal microtubule-binding domains and variable N-terminal domains. Mol Cell Biol 9:1381–1388.

Hirokawa N. 1994. Microtubule organization and dynamics dependent on microtubule- associated proteins. Curr Opin Cell Biol 6:74–81.

Hutton M, Lendon CL, Rizzu P, Baker M, Froelich S, Houlden H, Pickering-Brown S, Chakraverty S, Isaacs A, Grover A, Hackett J, Adamson J, Lincoln S, Dickson D, Davies P, Petersen RC, Stevens M, de Graaff E, Wauters E, van Baren J, Hillebrand M, Joosse M, Kwon JM, Nowotny P, Che LK, Norton J, Morris JC, Reed LA, Trojanowski J, Basun H, Lannfelt L, Neystat M, Fahn S, Dark F, Tannenberg T, Dodd P, Hayward N, Kwok JBJ, Schofield PR, Andreadis A, Snowden J, Craufurd D, Neary D, Owen F, Oostra BA, Hardy J, Goate A, van Swieten J, Mann D, Lynch T, Heutink P. 1998. Association of missense and 5′ splice site mutations in tau with the inherited dementia FTDP-17. Nature 393:702–705.

Ikegami S, Harada A, Hirokawa N. 2000. Muscle weakness, hyperactivity, and impairment in fear conditioning in tau-deficient mice. Neurosci Lett 279:129–132.

Johnson GV, Seubert P, Cox TM, Motter R, Brown JP, Galasko D. 1997. The tau protein in human cerebrospinal fluid in Alzheimer's disease consists of proteolytically derived fragments. J Neurochem 68:430–433.

Kanai Y, Hirokawa N. 1995. Sorting mechanisms of tau and MAP2 in neurons: Suppressed axonal transit of MAP2 and locally regulated microtubule binding. Neuron 14: 421–432.

Kempf M, Clement A, Faissner A, Lee G, Brandt R. 1996. Tau binds to the distal axon early in development of polarity in a microtubule- and microfilament-dependent manner. J Neurosci 16:5583–5592.

Kosik KS, Orecchio LD, Bakalis S, Neve RL. 1989. Developmentally regulated expression of specific tau sequences. Neuron 2:1389–1397.

Lee G, Neve RL, Kosik KS. 1989. The microtubule binding domain of human tau protein. Neuron 2:1615–1624.

Lee G, Newman ST, Gard DL, Band H, Panchamoorthy G. 1998. Tau interacts with src-family non-receptor tyrosine kinases. J Cell Sci 111:3167–3177.

Liu CW, Lee G, Jay DG. 1999. Tau is required for neurite outgrowth and growth cone motility of chick sensory neurons. Cell Motil Cytoskel 43:232–242.

LoPresti P, Szuchet S, Papasozomenos SC, Zinkowski RP, Binder LI. 1995. Functional implications for the microtubule-associated protein tau: Localization in oligodendrocytes. Proc Natl Acad Sci USA 92:10369–10373.

Lovestone S, Reynolds CH. 1997. The phosphorylation of tau: A critical stage in neurodevelopment and neurodegenerative processes. Neuroscience 78:309–324.

Lu PJ, Wulf G, Zhou XZ, Davies P, Lu KP. 1999. The prolyl isomerase Pin1 restores the function of Alzheimer-associated phosphorylated tau protein. Nature 399: 784–788.

Luo M, Memmott J, Andreadis A. 2004. Novel Isoforms of Tau that lack the microtubule-binding domain. Submitted.

Maccioni RB, Tapia L, Cambiazo V. 1995. Functional organization of tau proteins during neuronal differentiation and development. Braz J Med Biol Res 28:827–841.

Mandelkow EM, Biernat J, Drewes G, Gustke N, Trinczek B, Mandelkow E. 1995. Tau domains, phosphorylation, and interactions with microtubules. Neurobiol Aging 16: 355–362.

Nuydens R, Dispersyn G, de Jong M, van den Kieboom G, Borgers M, Geerts H. 1997. Aberrant tau phosphorylation and neurite retraction during NGF deprivation in PC12 cells. Biochem Biophys Res Commun 240:687–691.

Nuñez J, Fischer I. 1997. Microtubule-associated proteins MAPs in the peripheral nervous system during development and regeneration. J Mol Neurosci 8:207–222.

Poorkaj P, Kas A, D'Souza I, Zhou Y, Pham Q, Stone M, Olson MV, Schellenberg GD. 2001. A genomic sequence analysis of the mouse and human microtubule-associated protein tau. Mamm Genome 12:700–712.

Sayas CL, Moreno-Flores MT, Avila J, Wandosell F. 1999. The neurite retraction induced by lysophosphatidic acid increases Alzheimer's disease-like Tau phosphorylation. J Biol Chem 274:37046–37052.

Spillantini MG, Murrell JR, Goedert M, Farlow MR, Klug A, Ghetti B. 1998. Mutation in the *tau* gene in familial multiple system tauopathy with presenile dementia. Proc Natl Acad Sci USA 95:7737–7741.

Teng KK, Georgieff IS, Aletta JM, Nuñez J, Shelanski ML, Greene LA. 1993. Characterization of a PC12 cell subclone (PC12-C41) with enhanced neurite outgrowth capacity: Implications for a modulatory role of high molecular weight tau in neuritogenesis. J Cell Sci 106: 611–626.

Uberti D, Rizzini C, Spano PF, Memo M. 1997. Characterization of tau proteins in human neuroblastoma SH-SY5Y cell line. Neurosci Lett 235:149–153.

Wang Y, Loomis PA, Zinkowski RP, Binder LI. 1993. A novel tau transcript in cultured human neuroblastoma cells expressing nuclear tau. J Cell Biol 121:257–267.

Wei ML, Andreadis A. 1998. Splicing of a regulated exon reveals additional complexity in the axonal MAP tau. J Neurochem 70:1346–1356.

Wei ML, Memmott J, Screaton G, Andreadis A. 2000. The splicing determinants of a regulated exon in the axonal MAP tau reside within the exon and in its upstream intron. Brain Res Mol Brain Res 80:207–218.

Zhang J, Johnson GV. 2000. Tau protein is hyperphosphorylated in a site-specific manner in apoptotic neuronal PC12 cells. J Neurochem 75:2346–2357.

Zhao Z, Ho L, Suh J, Qin W, Pyo H, Pompl P, Ksiezak-Reding H, Pasinetti GM. 2003. A role of P301L tau mutant in anti-apoptotic gene expression, cell cycle and apoptosis. Mol Cell Neurosci 24:367–379.